OPEN

Under- and over-water halves of *Gyrinidae* beetle eyes harbor different corneal nanocoatings providing adaptation to the water and air environments

Artem Blagodatski[1], Michail Kryuchkov[1], Anton Sergeev[2], Andrey A. Klimov[3], Maxim R. Shcherbakov[4], Gennadiy A. Enin[1] & Vladimir L. Katanaev[1,5]

[1]Institute of Protein Research, Russian Academy of Sciences, Pushchino, Russian Federation, [2]Institute of Mathematical Problems of Biology, Russian Academy of Sciences, Pushchino, Russian Federation, [3]Institute of Theoretical and Experimental Biophysics, Russian Academy of Sciences, Pushchino, Russian Federation, [4]Faculty of Physics, Lomonosov Moscow State University, Moscow, Russian Federation, [5]Department of Pharmacology and Toxicology, University of Lausanne, Lausanne, Switzerland.

Whirligig beetles (*Gyrinidae*) inhabit water surfaces and possess unique eyes which are split into the overwater and underwater parts. In this study we analyze the micro- and nanostructure of the split eyes of two *Gyrinidae* beetles genera, *Gyrinus* and *Orectochilus*. We find that corneae of the overwater ommatidia are covered with maze-like nanostructures, while the corneal surface of the underwater eyes is smooth. We further show that the overwater nanostructures possess no anti-wetting, but the anti-reflective properties with the spectral preference in the range of 450–600 nm. These findings illustrate the adaptation of the corneal nanocoating of the two halves of an insect's eye to two different environments. The novel natural anti-reflective nanocoating we describe may find future technological applications.

Whirligig beetles (*Gyrinidae*) are a family of aquatic insects capable of diving and flying but spending most of their time on the water surface, half emerged. These beetles inhabit fresh and salty waters. Their name comes from their habit to change swimming directions very quickly and to move in circular patterns. Another remarkable feature of these beetles is the split structure of their compound eyes, which are divided into the overwater and underwater parts actually forming two independent eyes on each side of the head (Fig. 1)[1,2]. Such eye organization is an adaptation to the beetles' way of life, allowing the insects to observe objects both under water and above the surface. This adaptation is explainable for an animal occupying an ecological niche between two biotopes and needing to be equipped with a capacity of facing both of them. Similar evolutionary adaptations can be found in vertebrates like a fish species *Anableps anableps* which also possesses a pair of eyes split into the overwater and underwater halves[3]. However, optical properties of the air and the water are different, so one could expect a difference in the overwater and underwater eye anatomy in whirligig beetles. Although recent studies have revealed a peculiar way of organization of the visual brain centers in *Gyrinidae* to accommodate the split eye vision of these insects[4], the overall morphology and organization of the two eye portions is remarkably similar[5,6]. This suggests that finer aspects of the over- and under-water eyes of whirligig beetles, escaping previous analyses, may be present to accommodate the different optical requirements.

It is known that compound eyes of many insects harbor diverse nanostructures on the lens surface. Such nanostructures have been examined by means of electron and atomic force microscopy (AFM) in moths and butterflies[7–10] and our recent work describes the organization of nipple-formed nanostructures on the surface of the *Drosophila* eye[11]. Proposed functions of such insect nanostructures are anti-reflective, dirt-removing/self-cleaning, and hydrophobic/anti-wetting, and have inspired numerous industrial applications[9,12–18]. While the corneal nanocoating of many *Lepidopteran* and *Dipteran* insects is represented by pseudo-regular packaging of nipples[7–11], corneal surface of *Coleoptera* (the beetles) can be smooth or covered with irregular reticulations[8,19–21].
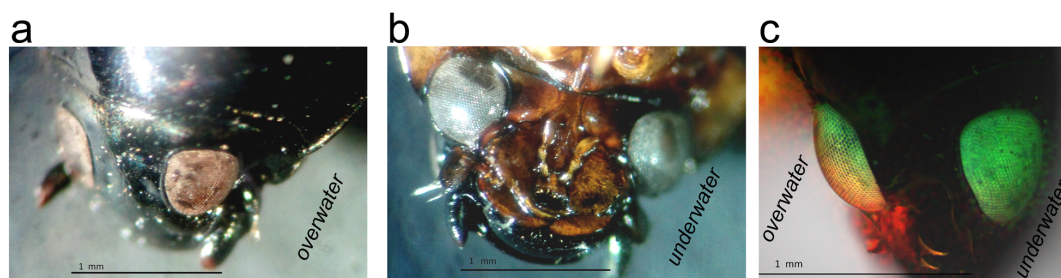
Figure 1 | The split eyes of the whirligig beetle *Gyrinus sp.* (a), (b), Top (a) and bottom (b) view of the head of *Gyrinus sp.* under a light microscope shows the overwater and the underwater eyes, respectively. (c), 3D-reconstruction of a lateral view of a *Gyrinus* beetle head taken by a fluorescent microscope; the overwater part is left and the underwater part is right.

Given the different environments – air vs. water – the two eye halves of the *Gyrinidae* beetles face, we suspected that their corneae may be armored with different surface nanostructures, fulfilling different requirements for e.g. the anti-wetting and anti-reflective functions. Here we analyze for the first time the nanostructures of whirligig corneae and discover the novel maze-like nanocoating of the overwater whirligig eyes, while the underwater eye corneae are smooth. We further show that these nanostructures provide no anti-wetting, but the anti-reflective function. As the morphology of the two eye halves is very similar[5,6], our studies provide the first example when the anti-reflective properties of nanocoated surface are compared with the 'natural control' – structure-less corneae of the underwater eye. The new anti-reflective maze-like nanostructures we describe may inspire future industrial applications.

Results

To analyze the morphology of the whirligig eye surfaces, we chose beetles belonging to two different genera of the *Gyrinidae* family, namely *Gyrinus* and *Orectochilus*. These beetles are common inhabitants of lakes, ponds and small rivers in Middle Russia. First, light and fluorescent microscopy images of the beetles' heads were made (Fig. 1); then the microstructure of the eyes was analyzed by means of AFM, depicting the ommatidial structure of the beetles' eyes (Fig. 2a, b). AFM inspection of individual lenses showed that the lens surface of the underwater eyes did not carry any nanoscale structures, but a structured surface could be observed on ommatidia of the overwater eyes (Fig. 2c, d).

Higher-resolution AFM analysis confirmed a smooth surface of the underwater eyes' corneae, except for chaotic scratches resulting from random mechanical damage; instead, complex maze-like nanostructures with the height of 20–30 nm were seen on the corneal surface of the overwater eyes (Fig. 3a–f). These images, taken with magnification of tens of micrometers to tens of nanometers, showed a clear difference in the corneal nanocoating of the overwater and underwater eyes of the *Gyrinus* beetles.

We repeated these analyses with a whirligig beetle of another genus, namely *Orectochilus sp*. The *Orectochilus* beetles share the ecological niche, way of life and behavior with the *Gyrinus* genus, so similar features were expected in corneal nanocoatings in both genera. And indeed, corneae of the overwater *Orectochilus* eyes demonstrated maze-like nanostructures on the surface, similar to that of the *Gyrinus* beetles, and the underwater eyes are structure-less except for random scratches (Fig. 3g, h).

The revealed difference in the corneal nanocoating morphology makes the *Gyrinidae* beetles a perfect object to study the functional role of these nanocoatings. The underwater and overwater eyes do not exhibit any other morphological differences (except for a slightly thicker dorsal cornea – ca. 27 µm versus ca. 22 µm on the ventral side)[2,5,6] thus the smooth underwater eye corneae may serve as a perfect control to measure physical properties of the nanocoated corneae of the overwater eyes. Such an internal natural control has always been lacking in previous analyses of the physical properties of insect nanostructures[8,15,22,23].

To assess whether not only the morphology of the dorsal and ventral whirligig eyes, but also the chemical composition of their corneal surfaces are similar, we analyzed them by Raman confocal microscopy – a powerful tool to assess the chemical composition of biological surfaces[24] with a potential to distinguish between different types of biological tissues and even between healthy and diseased tissues, when using an infrared laser[25]. The surface spectra obtained using an infrared laser (Fig. 4a) were almost identical for the underwater and overwater eyes corneae but differed drastically from a control *Drosophila* spectrum, thus giving a strong argument in favor of the chemical identity of the whirligig corneal samples.

Thus we compared the upper and lower eyes of *Gyrinus* beetles with regard to their wettability and light reflection – the two functions easily anticipated for the corneal nanocoating of water surface-inhabiting insects.

Our first hypothesis was that the whirligig eye nanostructures may affect wettability. Nipple nanoarrays covering cicada wings possess anti-wetting properties[15,16] but are higher (200–400 nm) than the ridges of the whirligig nanostructures. However, corneal nanostructures of ca. 20 nm in height of a butterfly have been described to render anti-adhesive properties[17], and the general theory predicts that rough surfaces are more hydrophobic, if not superhydrophobic as in the case of surfaces with high regularly spaced nanostructures[26]. To analyze wettability of whirligig cornea, we performed a series of experiments where distilled water droplets of about 200–300 micrometers in diameter were planted upon underwater and overwater eye surfaces by means of a glass capillary (Fig. 4b, c). Then we captured images of droplets upon the eyes and measured the angles between the eye surface and the droplets to characterize the eye surface wettability (Fig. 4d). Analysis of the contact angles of the droplets placed on the surface of the overwater and the underwater eyes, measured from both sides of the droplet, produced virtually identical data: $87.1°$ and $87.1°$ (right and left angles, respectively) for the upper eyes and $86.6°$ and $85.3°$ for the lower eyes (Fig. 4c). Thus, the overwater and underwater eyes are hydrophobic[26] – probably due to the chemical nature of the lens material – but possess similar anti-wetting properties, rejecting the hypothesis about the anti-wetting effect of the maze-like corneal nanocoatings of the whirligig upper eyes.

To analyze the possible differences in the light reflectance we performed another series of experiments, where we spotlighted the external surface of overwater and underwater eye cornea of *Gyrinus* beetles by a light emission diode and recorded them on a camera mounted on an optical microscope (Fig. 4e, f). The images were then analyzed to compare the percentage of the area of the reflected light patches within the total area of illuminated ommatidia. This analysis revealed a two-fold broader area of the reflected light patches for the underwater eye over the nanocoated overwater eye surface (Fig. 4g).

To exclude the possibility that this result may be influenced by the curvature of the lens, we performed an additional experiment acquir-
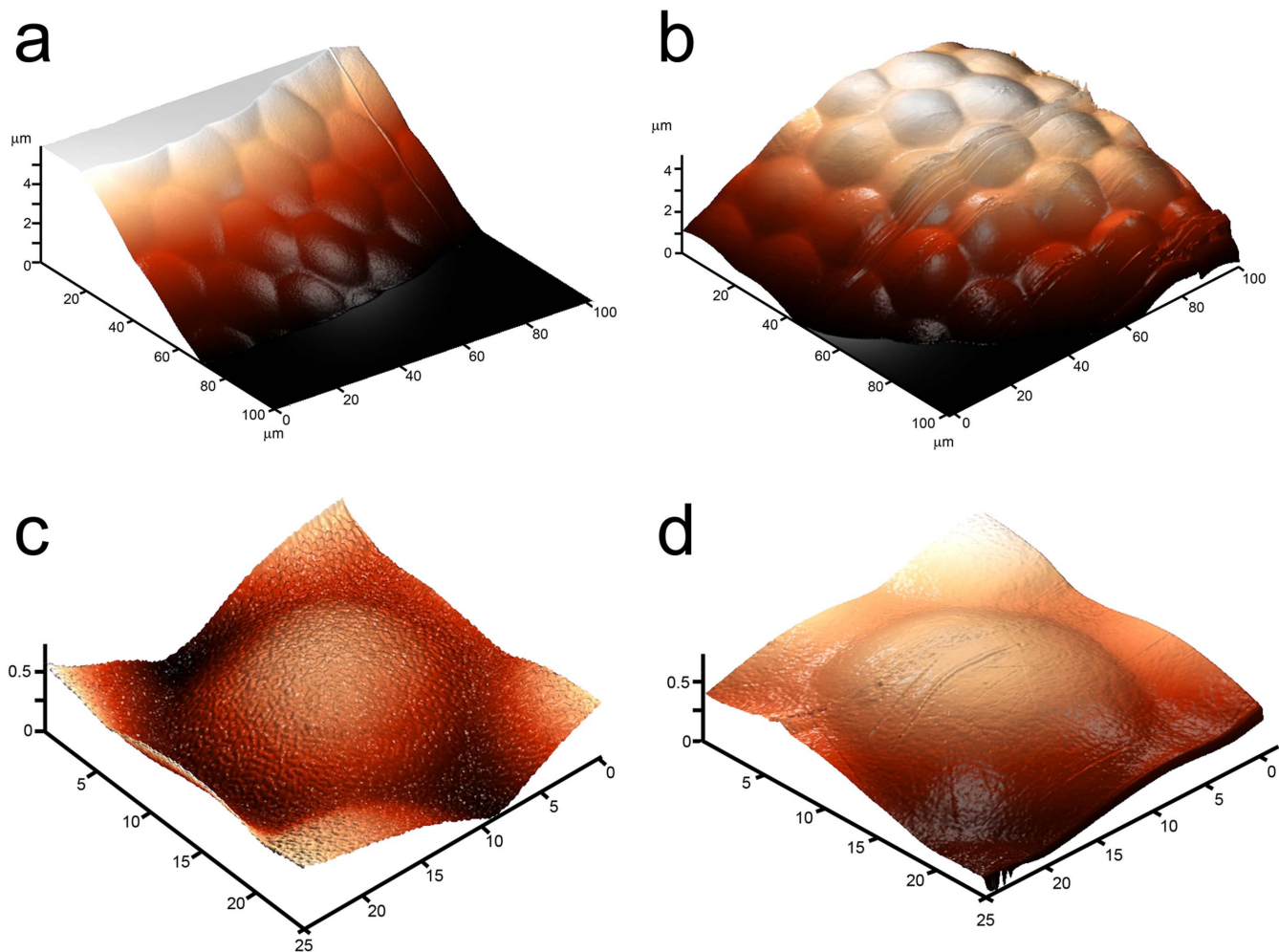
Figure 2 | Corneal surfaces of the overwater and the underwater eyes of *Gyrinus sp*. (a), (b), The overwater (a) and the underwater (b) eye microstructure of *Gyrinus sp*. seen by AFM depicts the ommatidial arrangements. (c), (d), 3D-images of corneal nanostructure of a single ommatidial lens of the overwater (c) and underwater (d) eyes of *Gyrinus sp* seen by AFM; a nanostructural coating can be detected on cornea of the overwater eye while the underwater eye cornea is smooth.

ing the reflectance with a high-numerical aperture (NA) objective which collects almost all of the total reflected light regardless of the curvature of the sample. In this analysis, we focused on individual ommatidia from the under- and over-water eyes. Furthermore, we analyzed the reflected light by a grating spectrometer, thus allowing us to determine the spectral characteristics of reflected light. Fig. 4h shows the ratio of the overwater-to-underwater eye reflection spectra. In this measurement, we see a consistently lower reflectance from the nanocoated overwater eye surface throughout most of the visible spectrum (450 to 600 nm); however, the reflective properties of the two eyes equalize in the red part of the spectrum (600–750 nm, Fig. 4h).

Thus, our study describes a novel maze-like nanocoating of whirligig corneae, possessing an anti-reflective function.

Discussion

In this article we for the first time provide an analysis of the corneal nanocoating of whirligig beetles, comparing their underwater and overwater eye halves. While the underwater corneae are smooth, the overwater ones carry maze-like nanostructures of ca. 20–30 nm in height. These structures do not change the hydrophobic properties of the corneae, but render them with an anti-reflective property throughout most of the visible spectrum. In the red part of the spectrum, the reflective properties of the underwater and overwater eyes equalize, which can be explained by a better sensitivity of the insect

eyes to the light of shorter wavelengths. The anti-reflective properties provided by the maze-like nanostructures likely serve to improve the optical properties of the whirligig overwater eyes. The anti-reflection effect of corneal nanocoatings is achieved by gradually matching the refractive index of the air to that of the lens material[11]. As the refractive index of the water is closer to that of the lens, no necessity for the nanostructures on the water-emerged corneae exists, explaining the smooth surface of whirligig underwater eyes.

Unlike most previous studies describing the anti-reflective effect of *Dipteran* and *Lepidopteran* eye nanocoating based upon theoretical[9] or artificial[27,28] models, we here demonstrate an important and direct experimental evidence for it in whirligig beetles. The earlier comparative light transmission and reflection measurements on insect corneae were performed only by matching corneal fragments from insects with nippled and insects with non-nippled facets[8,23], which could bear other morphological and chemical differences affecting reflectivity, while we were using benefits of comparing anti-reflective properties of overwater and underwater eyes of the same insect, having no differences[2,5,6] except for the nanocoatings.

The physical mechanism by which the pseudo-regular arrays of nano-nipples of *Dipterans* and *Lepidopterans* provide the anti-reflective function is quite clear[11], and the effect of height and shape of the nipples on the reflection properties can be modeled[8,29]. In contrast, the anti-reflective "beetle-eye" effect described here is provided by the maze-like corneal nanocoatings, for which the detailed
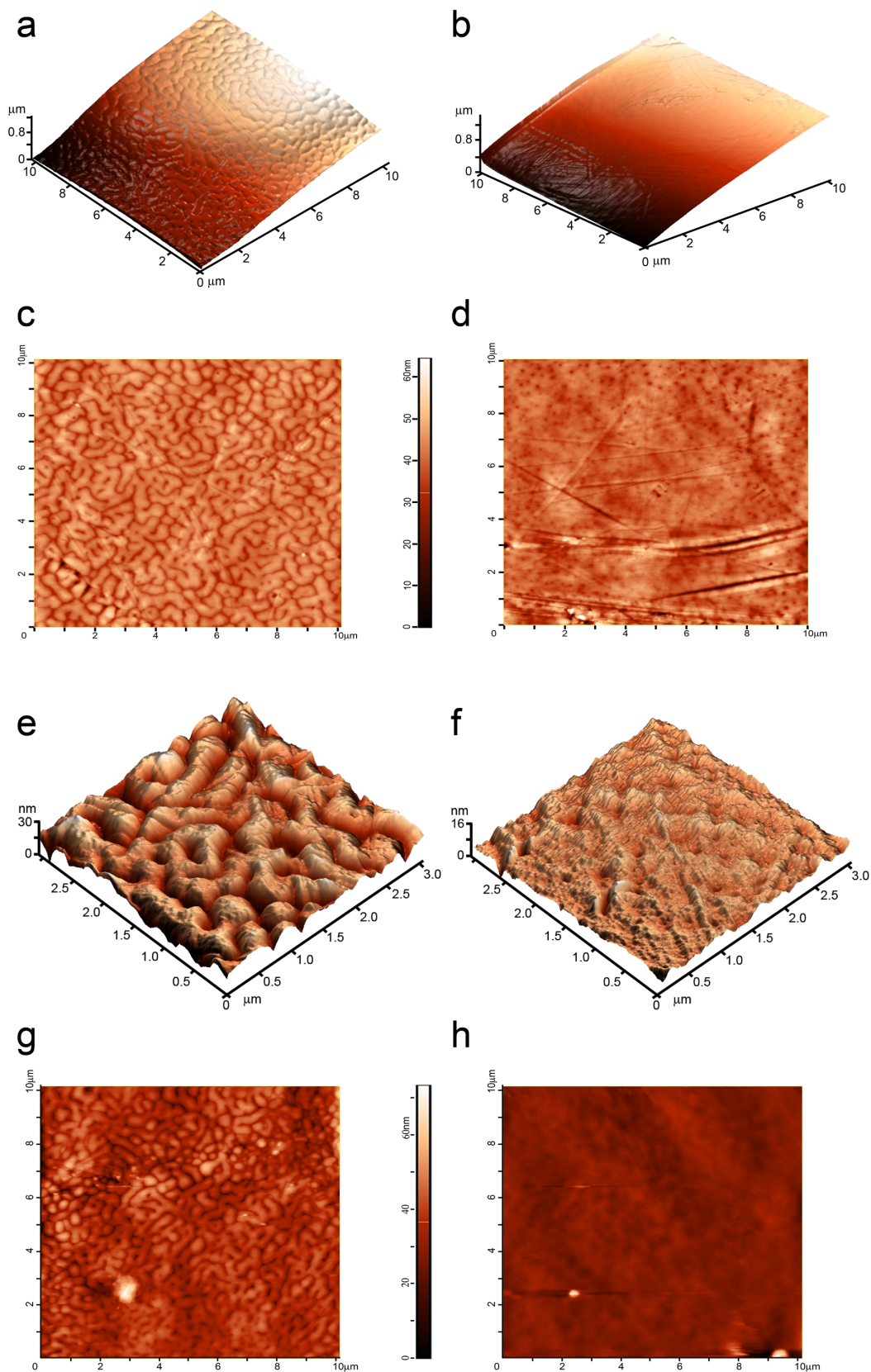
Figure 3 | The overwater and the underwater eyes of whirligig beetles display different corneal nanocoating. (a–d), AFM-based 3D- (a, b) and 2D-images (c, d) of 10 × 10 µm squares of the corneal surface of the overwater (a, c) and the underwater (b, d) eyes of *Gyrinus sp.* (e), (f), 3D-reconstruction of 3 × 3 micrometer squares of the corneal surface of the overwater (e) and the underwater (f) eyes of *Gyrinus sp.* Note different Z-axis scale of (e) and (f). (g), (h), 2D images of 10 × 10 µm corneal patches of the overwater (g) and the underwater (h) eyes of an *Orectochilus sp.* beetle. A complex maze-like nanocoating can be seen on the overwater eye corneae of both whirligig species, whereas no specific pattern is detectable on the underwater eye surface. Surface height is indicated by the color scale shown next to 2D-images.
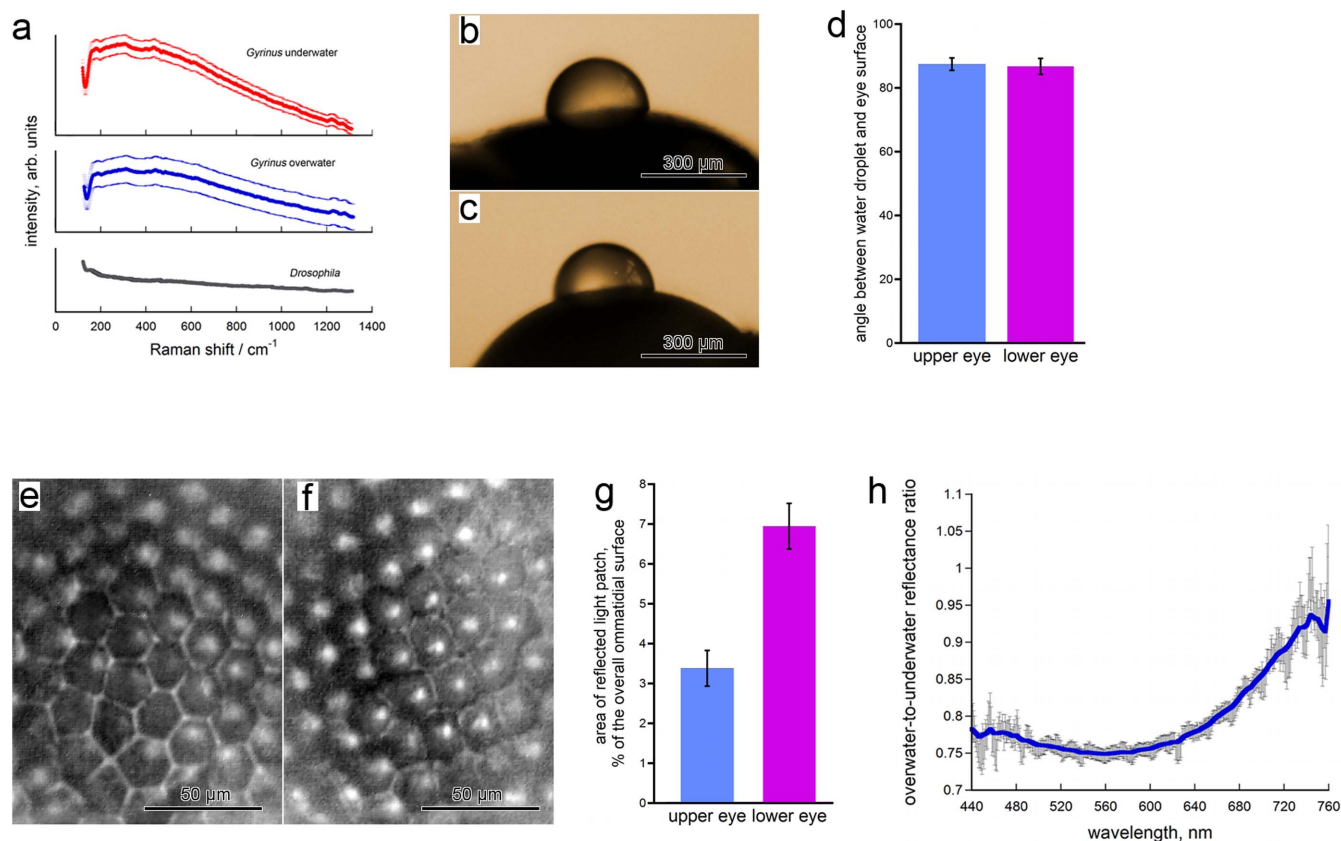
Figure 4 | The whirligig beetle corneal nanocoatings provide anti-reflective, but not anti-wetting function. (a), Raman spectra of the corneae of a underwater (red) and overwater (blue) ommatidia of a *Gyrinus* beetle specimen. The two spectra are almost identical and are very different from the spectrum of *Drosophila* corneae (gray). Data are shown as mean with the s.e.m. corridor from 3–4 different ommatidia. (b), (c), Droplets of water on surface of overwater (b) and underwater (c) eyes of a *Gyrinus* beetle. (d), The angles between the water droplet and the eye surface show no significant difference (p-value = 0.8352 by the Student t-test) in case of overwater and underwater eyes. Data are present as mean ± sem, n = 9. (e), (f), Light reflected from corneal surface of the overwater (e) and underwater (f) eyes, observed under optical microscope. Bright patches of reflected light could be seen on the illuminated underwater surface. (g), Calculation of the reflected light patch surface in relation to the bulk ommatidial surface for overwater and underwater eyes confirms a significant (p value < 0.0001 by the Student t-test) difference in the reflective properties of the two eyes. Data are present as mean ± sem, n = 12. (h), Ratio of the reflectance microspectra measured for over- and under-water eyes of *Gyrinus sp.* Signal reflected from seven adjacent ommatidia was spatially separated using a field stop and a high-NA objective. The antireflective effect of the overwater eye surface can be seen at wavelengths of 450–600 nm. The error bars reflect standard deviation. The image is a representative of analysis of five different beetles.

description of the physical principles as well as modeling has not yet been performed. Our studies illustrate an intriguing adaptation of the corneal nanocoating of the two halves of insects' eyes to the two different environments they face and give a functional explanation for this morphological difference. The novel natural anti-reflective nanocoating of whirligig beetles described here may find future technological applications.

Methods

Insect specimens. The dried samples of *Gyrinidae* beetles from gen. *Gyrinus* and *Orectochilus* were obtained from a collection belonging to the Department of Entomology, Moscow State University. Fresh *Gyrinus* specimens were collected in ponds around the town of Pushchino, Moscow region. *Drosophila melanogaster* (line *yw*) was kept under standard laboratory conditions[11].

Light and fluorescent microscopy. The photographs were taken under a light binocular microscope (Stemi 2000, Zeiss) with 64× magnification. The merged 3D image was obtained by using the "Z-stack" option of the Keyence BZ-9000 fluorescent microscope.

Atomic force microscopy. To prepare corneal samples from freshly captured specimens, the head of a whirligig beetle was severed from the body, followed by removal of the mouth apparatus with a scalpel, splitting of the head into two hemispheres, and careful extraction of the brain tissue with forceps. Next, the cornea was cleared from the head capsule tissue as well as the underlying brain material with a scalpel. The sample was attached to a glass slide for AFM by means of a two-sided scotch tape. AFM scanning of the lens was performed with the Integra-Vita microscope (NT-MDT, Zelenograd, Russia). For the semi-contact procedure, the nitride silicon cantilever NSG 03 (NT-MDT) was used. The parameters of the cantilever were: length: 100 µm, resonant frequency: 62–123 kHz, radius: 10 nm, force constant: 0.4–2.7 N/m. For the contact procedure, the cantilever CSG 10 (NT-MDT) was used, with the following parameters: length: 250 µm, resonant frequency: 14–28 kHz, radius: 10 nm, force constant: 0.03–0.2 N/m. The choice between the semi-contact and the contact measuring procedures was dictated by the size and curvature of the studied surface of the sample, but provided essentially identical results. In each AFM experiment several scans were made to check the reproducibility of images and the absence of possible surface damages.

Raman spectroscopy. The surface spectra of insect corneal samples were obtained by means of a Raman confocal microscope (Renishaw inVia) using a 785 nm infrared laser and a 100× objective. Three to four individual ommatidia were analyzed for the *Gyrinus* underwater and overwater eyes, as well as for *Drosophila melanogaster* eyes as a control.

Measurement of anti-wetting properties. The measurement was performed using a digital camera mounted upon a horizontally oriented optical microscope. Water droplets were planted upon beetle eyes with Narishige GD-1 glass capillaries held by Narishige MN-4 micromanipulator. After droplet planting upon the eye surface the images were captured and analyzed with the DropShape software; the mount level was set manually, the droplet circuits and contact angles were calculated automatically. The contact angles were measured from both sides of the droplet. The underwater and overwater eyes of three individual beetles were analyzed, with three independent experiments for each eye. The obtained data was processed by the Ooo-dev 3.4 Calc software to determine the standard error.

Measurement of light reflectance. The samples of underwater and overwater corneae were separated from the beetle eyes and mounted upon a slide by means of adhesive film, external surface facing up. Then they were spotlighted by a white light-emitting diode, 50 mA, 6000 K, and videos were captured by a digital camera mounted upon an optical microscope. To reduce background, 290 frames were stacked together for each video using the ImageJ software. Resulting images were then processed by the GIMP 2.8 software: the percent of the area covered by reflected light patches was determined in relation to the total area of all undamaged ommatidial lenses in focus; interommatidial spaces were not included into the analysis. Reflected light patches were defined as any spot with brightness higher than 200 relative units. Overwater and underwater corneal samples of total 6 independent *Gyrinus* specimens were analyzed, with 2 videos for each sample focused on different sample regions. The obtained data was processed by the Ooo-dev 3.4 Calc software to determine the standard error.

The reflectance of the beetle cornea in individual ommatidia was measured using the visible light microspectroscopy technique. The samples of underwater and overwater eyes were mounted on glass slides by means of an adhesive film, external surface facing down. The slide was placed on the sample stage of an inverted microscope (Lomo MIM-7 microscope with a 100× dry bright-field objective with NA = 0.85). The microscope was equipped with a custom white light-emitting diode source with enhanced radiance in the blue and near-UV ranges. The field stop was adjusted so that the cornea of a single ommatidium was illuminated by unpolarized light. The reflected light was collected with the same objective and focused onto the input of a multimode optical fiber coupled to a grating spectrometer (Solar LS S100). The output plane of the spectrometer was equipped with a 1024 pixel CCD line array (Hamamatsu) providing the spectral measurements in the range from 200 nm to 1000 nm with 0.9 nm resolution. The spectra were measured subsequently for the over- and under-water eyes, and then the ratio of the spectra intensities was calculated. This procedure was repeated at least three times for each eye pair in order to cancel the beam positioning ambiguity out. The overwater-to-underwater ratio spectra were smoothed by the adjacent-averaging filter of OriginLab Origin 7 software; this procedure reduces the spectral resolution to the value of 7-10 nm, which is not critical given the fact that the spectral dispersion of the reflectance manifests itself on larger spectral scales.

1. Hatch, M. H. The morphology of Gyrinidae. *Pap Mich Acad Sci Arts Lett.* **7**, 311–350 (1927).
2. Bott, H. R. Beiträge zur kenntnis von gyrinus natator substriatus steph. I. Lebensweise und entwicklung. II. Der sehapparat. *Z Morphol Oekol Tiere* **10**, 207–306 (1928).
3. Schwab, I. R., Ho, V., Roth, A., Blankenship, T. N. & Fitzgerald, P. G. Evolutionary attempts at 4 eyes in vertebrates. *Trans Am Ophthalmol Soc.* **99**, 145–156; discussion 156–147 (2001).
4. Lin, C. & Strausfeld, N. J. A precocious adult visual center n the larva defines the unique optic lobe of the split-eyed whirligig beetle Dineutus sublineatus. *Front Zool.* **10**, 7 (2013).
5. Horridge, G. A. & Giddings, C. Movement on Dark-Light Adaptation in Beetle Eyes of the Neuropteran Type. *Proc R Soc Lond B Biol Sci.* **179**, 73–85 (1971).
6. Wachmann, E. & Schröer, W.-D. Zur Morphologie des Dorsal- und Ventralauges des TaumelkäfersGyrinus substriatus (Steph.) (Coleoptera, Gyrinidae). *Zoomorphologie* **82**, 43–61 (1975).
7. Bernhard, C. G. & Miller, W. H. A corneal nipple pattern in insect compound eyes. *Acta Physiol Scand.* **56**, 385–386 (1962).
8. Bernhard, C. G., Gemne, G. & Sällström, J. Comparative ultrastructure of corneal surface topography in insects with aspects on phylogenesis and function. *J Comp Physiol A Neuroethol Sens Neural Behav Physiol.* **67**, 1–25 (1970).
9. Stavenga, D. G., Foletti, S., Palasantzas, G. & Arikawa, K. Light on the moth-eye corneal nipple array of butterflies. *Proc Biol Sci.* **273**, 661–667 (2006).
10. Watson, G. S. & Watson, J. A. Natural nano-structures on insects--possible functions of ordered arrays characterized by atomic force microscopy. *Appl Surf Sci.* **235**, 139–144 (2004).
11. Kryuchkov, M. *et al.* Analysis of micro- and nano-structures of the corneal surface of Drosophila and its mutants by atomic force microscopy and optical diffraction. *PLoS One* **6**, e22237 (2011).
12. Palasantzas, G., De Hosson, J. T. M., Michielsen, K. F. L. & Stavenga, D. G. Optical properties and wettability of nanostructured biomaterials: moth eyes, lotus leaves, and insect wings. in *Handbook of nanostructured biomaterials and their applications in nanobiotechnology*, Vol. 1. (ed. Nalwa, H. S.) 273–301 (American Scientific Publishers, 2005).
13. Park, K. C. *et al.* Nanotextured silica surfaces with robust superhydrophobicity and omnidirectional broadband supertransmissivity. *ACS Nano* **6**, 3789–3799 (2012).
14. Dewan, R. *et al.* Studying nanostructured nipple arrays of moth eye facets helps to design better thin film solar cells. *Bioinspir Biomim.* **7**, 016003 (2012).
15. Watson, G. S., Myhra, S., Cribb, B. W. & Watson, J. A. Putative functions and functional efficiency of ordered cuticular nanoarrays on insect wings. *Biophys J.* **94**, 3352–3360 (2008).
16. Sun, M. *et al.* Influence of cuticle nanostructuring on the wetting behaviour/states on cicada wings. *PLoS One* **7**, e35056 (2012).
17. Peisker, H. & Gorb, S. N. Always on the bright side of life: anti-adhesive properties of insect ommatidia grating. *J Exp Biol.* **213**, 3457–3462 (2010).
18. Huang, Y. F. *et al.* Improved broadband and quasi-omnidirectional anti-reflection properties with biomimetic silicon nanostructures. *Nat Nanotechnol.* **2**, 770–774 (2007).
19. Mishra, M. & Meyer-Rochow, V. B. Eye ultrastructure in the pollen-feeding beetle, Xanthochroa luteipennis (Coleoptera: Cucujiformia: Oedemeridae). *J Electron Microsc (Tokyo)* **55**, 289–300 (2006).
20. Chu, H., Norris, D. M. & Carlson, S. D. Ultrastructure of the compound eye of the diploid female beetle, Xyleborus ferrugineus. *Cell Tissue Res.* **165**, 23–36 (1975).
21. Chu, H. M. & Norris, D. M. Ultrastructure of the compound eye of the haploid male beetle, Xyleborus ferrugineus. *Cell Tissue Res.* **168**, 315–324 (1976).
22. Yoshida, A., Motoyama, M., Kosaku, A. & Miyamoto, K. Antireflective Nanoprotuberance Array in the Transparent Wing of a Hawkmoth, Cephonodes hylas. *Zool Sci.* **14**, 737–741 (1997).
23. Miller, W. H., Moller, A. R. & Bernhard, C. G. The corneal nipple array. in *The functional organization pf the compound eye.* (ed. Bernhard, C. G.) 21–33 (Pergamon Press, London; 1966).
24. Stewart, S., Priore, R. J., Nelson, M. P. & Treado, P. J. Raman imaging. *Annu Rev Anal Chem.* **5**, 337–360 (2012).
25. Wachsmann-Hogiu, S., Weeks, T. & Huser, T. Chemical analysis in vivo and in vitro by Raman spectroscopy--from single cells to humans. *Curr Opin Biotechnol.* **20**, 63–73 (2009).
26. Hsu, S.-H., Woan, K. & Sigmund, W. Biologically inspired hairy structures for superhydrophobicity. *Mat Sci Eng R.* **72**, 189–201 (2011).
27. Parker, A. R., Hegedus, Z. & Watts, R. A. Solar–absorber antireflector on the eye of an Eocene fly (45 Ma). *Proc R Soc Lond B Biol Sci.* **265**, 811–815 (1998).
28. Nakata, K. *et al.* Antireflection and self-cleaning properties of a moth-eye-like surface coated with TiO2 particles. *Langmuir* **27**, 3275–3278 (2011).
29. Dewan, R. *et al.* Studying nanostructured nipple arrays of moth eye facets helps to design better thin film solar cells. *Bioinspir Biomim.* **7**, 016003 (2012).

Acknowledgments

Author contributions

A.B. collected the samples, performed the wettability analysis and coordinated other analyses and wrote the paper; M.K. prepared the samples for and performed the microscopy analysis; A.S. performed AFM analysis; A.A.K. and M.R.S. performed the experiments on Figure 4; G.A.E. provided the AFM expertise; V.L.K. designed and coordinated the work and wrote the paper; all the authors additionally participated in the discussion of results.

Additional information